

The P -odd interaction constant W_A from relativistic *ab initio* calculations of diatomic molecules

A. Borschevsky,¹ M. Iliáš,² V. A. Dzuba,³ K. Beloy,¹ V. V. Flambaum,³ and P. Schwerdtfeger^{1,4}

¹*Centre for Theoretical Chemistry and Physics, The New Zealand Institute for Advanced Study, Massey University Auckland, Private Bag 102904, 0745 Auckland, New Zealand*

²*Department of Chemistry, Faculty of Natural Sciences, Matej Bel University, Tajovského 40, SK-974 00 Banská Bystrica, Slovakia*

³*School of Physics, University of New South Wales, Sydney 2052, Australia*

⁴*Fachbereich Chemie, Philipps-Universität Marburg, Hans-Meerwein-Str., D-35032 Marburg, Germany*

(Dated: July 5, 2019)

We present *ab initio* calculations of the W_A parameter of the P -odd spin-rotational Hamiltonian for a variety of diatomic molecules, including the group-2 and -12 halides. The results were obtained by relativistic Dirac-Hartree-Fock and density functional theory approaches, and corrected for core polarization effects. Strong enhancement of W_A is found for the group-12 diatomic halides, which should be helpful in future determination of the nuclear anapole moment.

PACS numbers: 37.10.Gh, 11.30.Er, 12.15.Mm, 21.10.Ky

I. INTRODUCTION

The anapole moment was predicted first by Zeldovich [1] in 1958 as a new parity violating (PV) and time reversal (T) conserving moment of an elementary particle. It appears in the second-order multipole expansion of the magnetic vector-potential simultaneously with the P - and T -violating magnetic quadrupole moment [2]. The nuclear anapole moment was experimentally discovered in the ^{133}Cs atom in 1997 [3]. This measurement was performed following a proposal by Flambaum and Khriplovich [4], who have shown that the nuclear anapole provides the dominant contribution to the nuclear-spin-dependent (NSD) parity violating effect in atoms and molecules. It can provide important information about hadronic weak coupling, which is currently not so easily obtained from first-principles nuclear structure calculations (e.g., see Ref. [5] and Review [6]). The term in the Hamiltonian operator arising from NSD parity violating electron-nucleus interaction is

$$H_A = \kappa_{NSD} \frac{G_F}{\sqrt{2}} \frac{\boldsymbol{\alpha} \cdot \mathbf{I}}{I} \rho(\mathbf{r}), \quad (1)$$

where κ_{NSD} is the dimensionless strength constant, $G_F = 2.22249 \times 10^{-14}$ a.u. is the Fermi constant, $\boldsymbol{\alpha}$ is a vector comprised of the conventional Dirac matrices, \mathbf{I} is the nuclear spin, \mathbf{r} is the displacement of the valence electron from the nucleus, and $\rho(\mathbf{r})$ is the (normalized) nuclear density. There are three sources for this interaction: the first contribution arises from the electroweak neutral coupling between electron vector and nucleon axial-vector currents ($\mathbf{V}_e \mathbf{A}_N$) [7]. The second contribution comes from the nuclear-spin-independent weak interaction combined with the hyperfine interaction [8]. Finally, the nuclear anapole moment contribution scales with the number of nucleons, A , with $\kappa_A \sim A^{2/3}$, and becomes the dominant contribution in spin-dependent atomic parity violation effects for sufficiently large nuclear charge Z [4, 9]. It requires nuclear spin $I \neq 0$ and

in a simple valence model has the following value [9]

$$\kappa_A = 1.15 \times 10^{-3} \left(\frac{\mathcal{K}}{I+1} \right) A^{2/3} \mu_i g_i, \quad (2)$$

Here, $\mathcal{K} = (-1)^{I+\frac{1}{2}-l}(I+1/2)$, l is the orbital angular momentum of the external unpaired nucleon $i = n, p$; $\mu_p = +2.8$, $\mu_n = -1.9$. Theoretical estimates give the strength constant for nucleon-nucleus weak potential $g_p \approx +4.5$ for a proton and $|g_n| \sim 1$ for a neutron [10]. The aim of anapole measurements is to provide accurate values for these constants. The nuclear anapole moment for ^{133}Cs ($I=7/2$), containing a single valence proton, was measured from the differences in the $6S_{F=4}$ to $7S_{F=3}$ and $6S_{F=3}$ to $7S_{F=4}$ hyperfine transitions as $\kappa_A = 364(62) \times 10^{-3}$ [3, 10]. However, the limit on g_p ($g_p = -2 \pm 3$ [6]), obtained from the Tl anapole measurements [11], seems to contradict the Cs anapole measurements ($g_p = 6 \pm 1$, see [10]). This indicates that further refinements in the experimental measurements are required to obtain high precision results for nuclear spin-dependent parity violation effects in atoms.

In Refs. [12–14] it was shown that the nuclear spin-dependent parity violation effects are enhanced by a factor of 10^5 in diatomic molecules with $^2\Sigma_{1/2}$ and $^2\Pi_{1/2}$ electronic states due to the mixing of close rotational states of opposite parity (Ω -doublet for $^2\Pi_{1/2}$). DeMille and co-workers suggested therefore to measure the anapole moment by using diatomic molecules in a Stark interference experiment to determine the mixing between opposite-parity rotational/hyperfine levels [15]. The molecular route opens up the range of systems to be studied and should provide data on anapole moments for many heavy nuclei. Another motivation comes from a possibility to test the standard model. The anapole moment contribution is small in light nuclei with a valence neutron (Eq. (2)). In this case the electroweak contribution may be extracted from the measurements of NSD PV effects [15]. This contribution has never been measured.

We therefore present Dirac-Hartree-Fock (corrected for electron correlation) and 4-component density functional theory calculations of the electronic factor W_A for the diatomic group-2 and -12 fluorides and a number of other diatomic compounds.

II. COMPUTATIONAL DETAILS.

For ${}^2\Sigma_{1/2}$ and ${}^2\Pi_{1/2}$ electronic states, the interaction (1) can be replaced by the effective operator, which appears in the spin-rotational Hamiltonian [14, 15],

$$H_A^{\text{eff}} = \kappa_{NSD} W_A \frac{(\mathbf{n} \times \mathbf{S}') \cdot \mathbf{I}}{I}, \quad (3)$$

where \mathbf{S}' is the effective spin (discussed below) and \mathbf{n} is the unit vector directed along the molecular axis from the heavier to the lighter nucleus.

Calculations of the P -odd interaction constant W_A were carried out within an open-shell single determinant average-of-configuration Dirac-Hartree-Fock approach (DHF) [16] and within the relativistic density functional theory (DFT) [17], employing quaternion symmetry [18, 19]. We used the DIRAC10 computational package [20] to perform all the calculations. The electronic factor W_A is found from evaluating the matrix elements of the $\alpha\rho(\mathbf{r})$ operator in the molecular spinor basis [21]. ${}^2\Sigma_{1/2}$ and ${}^2\Pi_{1/2}$ open-shell electronic states are two-fold degenerate, corresponding to the two possible projections of electronic angular momentum along \mathbf{n} , i.e. $|\Omega\rangle = |\pm \frac{1}{2}\rangle$. When operating within this degenerate space, the operator $\frac{G_F}{\sqrt{2}}\alpha\rho(\mathbf{r})$ is equivalent to $W_A(\mathbf{n} \times \mathbf{S}')$ (Eq. (3)). Time-reversal symmetry ensures that only the matrix elements that are off-diagonal in Ω are non-vanishing. This symmetry rule is encapsulated within the effective operator H_A^{eff} by the angular factor $(\mathbf{n} \times \mathbf{S}')$. Here the effective spin \mathbf{S}' generates rotations in the degenerate subspace analogously to usual spin operator \mathbf{S} in a spin-1/2 system. In the non-relativistic limit, $\mathbf{S}' \rightarrow \mathbf{S}$ for ${}^2\Sigma_{1/2}$ states. A finite nucleus, modelled by the Gaussian charge distribution was employed [22]. We note that a nuclear point charge approximation should be avoided in calculations of W_A as the resulting singularity in the wave function gives unphysical results.

In the DFT calculations we used the Coulomb-attenuated B3LYP functional, (CAMB3LYP*), the parameters of which were adjusted by Thierfelder *et al.* [23] to reproduce the PV energy shifts obtained using coupled cluster calculations. The newly adjusted parameters are $\alpha = 0.20$, $\beta = 0.12$, and $\mu = 0.90$. In order to test the stability of the results with respect to the choice of the functional, the calculations were performed also using the PBE, LDA, and B3LYP functionals. For all the systems the W_A parameters obtained using the different functionals were in remarkably good agreement, within up to $\sim 10\%$ (the only exception being RaF, where the LDA results were 15% higher than the CAMB3LYP* ones). We thus only present the CAMB3LYP* values,

which are considered to give the best results for parity violating properties [23].

For the lighter elements (N, O, F, Mg, and Cl), uncontracted aug-cc-pVTZ basis sets were used [24, 25]. For the rest of the atoms, we employed Faegri's dual family basis sets [26]. A good description of the electronic wave function in the nuclear region is essential for obtaining reliable results for parity violating properties [27]. Thus, we augmented the basis sets with high exponent s and p functions, which brings about an increase of around 10% in the calculated values of W_A . The basis sets were increased, both in the core and in the valence regions, to convergence with respect to the calculated W_A constants. The final basis sets can be found in the Appendix.

Where available, we used experimental geometries. For molecules where the bond length R_e is not known experimentally, we optimized the bond distance instead, using relativistic coupled cluster theory with single, double, and perturbative triple excitations (CCSD(T)) [28]. To reduce the computational effort, the Dirac-Coulomb Hamiltonian was replaced by an infinite order two-component relativistic Hamiltonian obtained after the Barysz-Sadlej-Snijders (BSS) transformation of the Dirac Hamiltonian in a finite basis set [29, 30]. Our calculated R_e are typically within 0.01 Å of the experimental values, where available. The experimental/calculated equilibrium distances can be found in Tables I and II.

Previous investigations for the BaF molecule have shown that the electron correlation contribution to the W_A constant is non-negligible, and raises its value by $\sim 20\text{-}50\%$ [32, 33]. In this work we use two separate schemes to account for the correlation effects: the density functional calculations, and correcting the DHF values for the correlation contributions using atomic calculations, in a manner outlined below.

The main contribution to the matrix elements of the NSD interaction for the valence molecular electrons comes from short distances around the heavy nucleus. Thus, these matrix elements are strongly affected by correlations between the core and the valence electrons.

The total molecular potential at short distances from the heavy nucleus is spherically symmetric to very high precision; the core of the heavy atom is practically unaffected by the presence of the second atom. The molecular orbitals of the valence electron can thus be expanded in this region, using spherical harmonics centered at the heavy nucleus,

$$|\psi_v\rangle = a|s_{1/2}\rangle + b|p_{1/2}\rangle + c|p_{3/2}\rangle + d|d_{3/2}\rangle \dots \quad (4)$$

Only $s_{1/2}$ and $p_{1/2}$ terms of this expansion give significant contribution to the matrix elements of the weak interaction. These functions can be considered as states of an atomic valence electron, and are calculated using standard atomic techniques in two different approximations: one that includes electron correlation and another that does not. The correlation factor K_{tot} is then defined as $K_{tot} = K_W \cdot K_{E1} \cdot K_{En}$. Here, K_W is found as the

TABLE I. Internuclear distances R_e (Å) and the P -odd interaction constants W_A (Hz) obtained on different levels of theory: DHF, DFT, DHF and DFT scaled for core polarization contribution, $DFT \cdot K_{CP}$ and $DHF \cdot K_{CP}$, DHF corrected for total correlation effect, $DHF \cdot K_{tot}$, and the final recommended values, taken as $W_A(\text{Final}) = (W_A(\text{DFT}) \cdot K_{CP} + W_A(\text{DHF}) \cdot K_{CP})/2$. Comparison with earlier results is also shown.

Nucleus		R_e (Å)	W_A (Hz)						Previous results		
			DFT	DHF	$DFT \cdot K_{CP}$	$DHF \cdot K_{CP}$	$DHF \cdot K_{tot}$	Final	W_A (Hz)	Method	Ref.
SrF	Sr	2.075 [31]	42	41	53	51	49	52	65	Semiempirical	[15]
MgBr	Br	2.360 [31]	18	9	24	11	11	18	18	Semiempirical	[15]
ZnN	Zn	1.696 [31]	56	63	67	76	70	72	99	Semiempirical	[15]
BaF	Ba	2.162 [31]	121	123	152	154	142	153	164	Semiempirical	[15]
									135	DHF	[32]
									160	4c-RASCI ^a	[32]
									111	RECP+ SCF+EO ^b	[33]
									181	RECP+RASSCF+EO ^c	[33]
									210-240	Semiempirical	[34]
LaO	La	1.825 [31]	161	164.3	197	201	186	199	222	Semiempirical	[15]
YbF	Yb	2.016 [31]	631	527	657	549	590	602	729	Semiempirical	[15]
									484	RECP+SCF	[35]
									486	RECP+RASSCF	[35]
HgF	Hg	2.025 ^d	3207	3557	3502	3884	3023	3693	2700	Semiempirical	[34]
PbF	Pb	2.078 [31]	-1382	-1349	-1517	-1481	-1200	-1499	-720	Semiempirical	[36]
									-950±300	Semiempirical	[37]
									-990	RECP+SODCI ^e	[38]
RaF	Ra	2.255 ^d	1681	1465	2054	1790	1773	1922	1300	ZORA+SCF ^f	[39]

^a Fully relativistic restricted active space configuration interaction method.

^b Relativistic effective core potential (RECP) combined with SCF and an effective operator to account for core-valence correlations.

^c RECP combined with restricted active space SCF approach and an effective operator to account for core-valence correlations.

^d CCSD(T), present calculations

^e RECP combined with spin-orbit direct configuration interaction

^f Quasirelativistic two-component zero-order regular approximation combined with the SCF approach.

ratio of the matrix elements

$$K_W = \frac{\langle ns'_{1/2} | \hat{H}'_A | np'_{1/2} \rangle}{\langle ns_{1/2} | \hat{H}_A | np_{1/2} \rangle} \quad (5)$$

where the matrix element in the numerator includes electron correlation, while the matrix element in the denominator does not. The magnitude of K_W is larger than 1, as the many body corrections due to correlation with the core electrons increase the density of the valence electron on the nucleus [40], and thus, increase the W_A constant.

Correlations also modify the expansion coefficients a , b , c , ... in Eq. (4). An estimate of this effect shows that it reduces the overall correlation contribution, and provides us with K_{E1} and K_{E_n} , corresponding to the effect of correlations on the $E1$ amplitude and on the orbital energies, respectively.

Multiplying the result of molecular DHF calculations by K_{tot} allows us to include the effect of the most important electron correlation contributions (Table I, $DHF \cdot K_{tot}$). The Appendix contains the details of the calculation and the values of K_{tot} for all the atoms studied here.

Core polarization effects are not accounted for in the Kramers restricted DFT calculations. These effects are included in K_{tot} ; however, we also examine their influence separately from the rest of the correlation contributions. Thus, we define an additional scaling factor, K_{CP} , which only takes the core polarization into account (see Appendix for the details of calculation and the values of K_{CP}). Table I contains the DHF and the DFT values, corrected for core polarization contribution ($DHF \cdot K_{CP}$ and $DFT \cdot K_{CP}$).

As the recommended value for the W_A parameter we take an average of $W_A(\text{DHF}) \cdot K_{CP}$ and $W_A(\text{DFT}) \cdot K_{CP}$, since we believe that these two values represent our most reliable results.

III. RESULTS AND DISCUSSION

All the systems under study have a single valence electron; the ground state of the PbF molecule is $^2\Pi_{1/2}$, the remaining molecules have a $^2\Sigma_{1/2}$ ground state. Table I contains the results obtained for molecules, for which earlier calculations were performed. For comparison, we present the uncorrelated DHF results, together with the different correlation schemes used: the DFT values, the DHF and the DFT values corrected for core polarization, the DHF values corrected for the overall correlation effects, $W_A(\text{DHF}) \cdot K_{tot}$, and the final recommended values. To the best of our knowledge, these are the first DFT calculations of W_A . The spread of the values obtained by different methods may be used to estimate the accuracy of our calculations, as the uncertainty of the result is strongly dominated by the correlation correction contribution. The difference between the DFT and DHF values gives us an estimate for the correlation contribution, which is included into DFT and absent in DHF. Another (and probably less accurate) method to estimate the correlations is to compare K_{CP} and K_{tot} . From these comparisons we have come to conclusion that the accuracy of W_A produced by the metal anapole moments is about 15% for Σ terms and 20-30% for $\Pi_{1/2}$ terms (such as PbF). The accuracy of W_A produced by Br (or other

TABLE II. Internuclear distances, R_e (Å), relativistic factors R_W , and the recommended values of W_A constants (Hz), taken as $W_A(\text{Final}) = (W_A(\text{DFT}) \cdot K_{CP} + W_A(\text{DHF}) \cdot K_{tot})/2$ for group-2 and -12 fluorides, and for mercury halides.

	Z	R_e (Å)	R_W	$W_A(\text{Final})$ (Hz)
Group-2 fluorides				
MgF	12	1.750 [31]	1.06	5
CaF	20	1.967 [31]	1.17	11
SrF	38	2.075 [31]	1.65	52
BaF	56	2.162 [31]	2.73	153
RaF	88	2.244 ^a	10.34	1922
Group-12 fluorides				
ZnF	30	1.766 [41]	1.38	64
CdF	48	1.991 ^a	2.14	264
HgF	80	2.025 ^a	7.03	3693
Mercury halides				
HgCl	80	2.387 ^a	7.03	3647
HgBr	80	2.468 ^a	7.03	3600
HgI	80	2.736 ^a	7.03	3356

^a CCSD(T), present calculations

halogen) anapole moment is about 30%.

Most of the previous investigations of W_A rely on semiempirical methods, while for BaF, YbF, RaF, and PbF *ab initio* calculations were also performed [32, 33, 35, 38, 39]. Our results are in good agreement with the recent semiempirical values for most of the systems; in case of HgF, PbF, and RaF our final W_A constants are higher than the previous values by about 30%.

For BaF we can compare our results to other *ab initio* calculations. Our DHF value is close to that of Nayak and Das [32], obtained by a similar method, and to that of Kozlov *et al.* [33], calculated by the combination of relativistic effective core potential (RECP) and the SCF approach, and corrected for valence-core correlation by an effective operator. The value of W_A corrected for correlation is in very good agreement with both the relativistic restricted active space configuration interaction (4c-RASCI) result of Ref. [32], and the RECP restricted active space SCF approach of [33].

Two other systems with *ab initio* results are YbF [35], calculated using a combination of RECP and SCF/RASCF methods, and RaF [39], treated via the quasirelativistic two-component zero-order regular approximation (ZORA) combined with an SCF approach. As both these investigations do not treat electron correlation, we can compare them directly to our DHF results, which are in good agreement.

Our correlated result for PbF is rather higher than that obtained in the previous investigation [38] performed using a combination of RECP and spin-orbit direct configuration interaction, which might be caused by the 4-component treatment of relativity in our case. This system is different from the other molecules discussed here, due to its ground state. For the $^2\Pi_{1/2}$ electronic state W_A vanishes in the non-relativistic limit, since in this limit it does not contain the s -wave electronic orbital and can

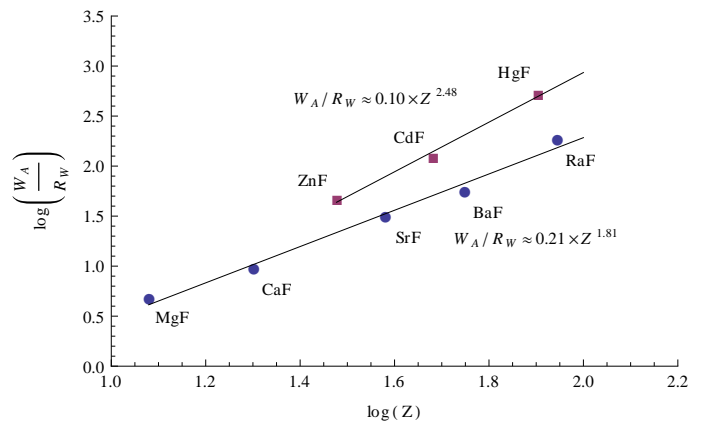


FIG. 1. Scaling of $\log\left(\frac{W_A}{R_W}\right)$ with $\log(Z)$ for group-2 and -12 fluorides

not provide the matrix element $\langle s_{1/2} | W_A | p_{1/2} \rangle$. The effect appears due to the mixing of $^2\Sigma_{1/2}$ and $^2\Pi_{1/2}$ electronic states by the spin-orbit interaction. This gives an extra factor of $Z^2\alpha^2$ in the Z -dependence of the matrix element of W_A in a $^2\Pi_{1/2}$ electronic state. This does not lead to a significant suppression in heavy molecules, such as PbF; however, in light molecules the matrix element of W_A in the $^2\Pi_{1/2}$ electronic state is much smaller than that in $^2\Sigma_{1/2}$ state (note that a similar factor $Z^2\alpha^2$ also makes the interval between the opposite parity Λ -doublet states small; therefore, there is actually no suppression in the mixing of these states by W_A).

Table II contains the recommended W_A constants for the group-2 and group-12 fluorides. The magnitude of W_A in $^2\Sigma_{1/2}$ electronic state is expected to scale as $Z^2 R_W$ [8], where R_W is the relativistic parameter,

$$R_W = \frac{2\gamma + 1}{3} \left(\frac{a_B}{2Zr_0 A^{1/3}} \right)^{2-2\gamma} \frac{4}{[\Gamma(2\gamma + 1)]^2}, \quad (6)$$

$$\gamma = [1 - (Z\alpha)^2]^{1/2}.$$

In Eq. (6), a_B is the Bohr radius, $r_0 = 1.2 \times 10^{-15}$ m, and α is the fine-structure constant. The R_W parameters are shown in Table II for each of the metal atoms. In Fig. 1 we plot $\log\left(\frac{W_A}{R_W}\right)$ as a function of $\log(Z)$ for both groups of dimers. For group-2 fluorides the scaling is, indeed, close to Z^2 ; however, the interesting feature of the plot is group-12 fluorides, where the Z -dependence is much more advantageous, of $Z^{2.5}$. This is due to the filling of the lower lying d -shell, which expands relativistically and thus increases the effective nuclear charge, leading to an enhancement of relativistic and PV effects [42], and an increase of W_A . It should be noted that measurements for W_A in MgF and CaF may be used to test the standard model, since the anapole moments of Mg and Ca are small and the electroweak contribution to NSD PV electron-nucleus interaction is important.

Table II also shows the W_A constants of mercury halides. The W_A values are very close for all the halo-

gens; the situation is similar for zinc and cadmium halides. However, molecules containing heavier ligands might have an experimental advantage. Due to the higher reduced mass, the interval between the opposite parity rotational levels becomes smaller, and thus larger PV effects can be expected, and a smaller magnetic field would be needed to reduce the interval between the levels.

Acknowledgements This work was supported by the Marsden Fund (Royal Society of New Zealand), the Australian Research Council and the Alexander von Humboldt Foundation (Bonn). MI is grateful for the financial support from the Slovak Research and Development Agency (grant number APVV-0059-10).

IV. APPENDIX

A. Basis sets

Table III contains the basis sets used in the calculations of the W_A constants. For the lighter elements (N, O, F, Mg, and Cl), uncontracted augmented correlation-consistent valence triple- ζ (AVTZ) Gaussian basis sets were used [24, 25]. For the rest of the atoms, we employed the Faegri's dual family basis sets [26], augmented with higher orbital momentum and diffuse functions. Good description of the electronic wave function in the nuclear region is essential for obtaining reliable results for parity violating properties [27]. Thus, we also augmented the basis sets with high exponent s and p functions, which brings about an increase of around 10% in the calculated values of W_A . The basis sets were increased, both in the core and in the valence regions, to achieve convergence with respect to the obtained W_A constants. The same basis sets were employed in the relativistic CCSD(T) geometry optimizations (where experimental geometry was unavailable). However, here we leave out the high exponent s and p functions, as these contribute little to molecular geometries.

B. Calculation of the correlation factors K_{CP} and K_{tot}

The scaling factors K_{CP} and K_{tot} are used for estimating the effect of the core polarization and of the overall correlation effects on W_A for the molecules. These factors are found using two sets of atomic calculations, one that neglects electron correlation and on that includes it. The calculations, and the derivation of the K_{CP} and K_{tot} factors are described below.

1. Atomic calculations without electron correlation

We use the relativistic Dirac–Hartree–Fock method (DHF) to perform atomic calculations [43]. In atomic

TABLE III. Basis sets employed in the calculation of the W_A constants. All elements with $Z > 17$ are described by the Faegri basis sets [26] augmented by high exponent, diffuse, and high angular momentum functions.

Atom	Z	Basis Set
N	7	aug-cc-PVTZ
O	8	aug-cc-PVTZ
F	9	aug-cc-PVTZ
Mg	12	aug-cc-PVTZ ^a
Cl	17	aug-cc-PVTZ
Ca	20	20s18p9d6f1g
Zn	30	21s19p10d7f2g
Br	35	21s20p10d10f1g
Sr	38	21s20p12d9f2g
Zr	40	21s20p12d9f2g
Cd	48	22s20p12d9f2g
I	53	22s21p12d11f2g
Ba	56	24s22p15d10f2g
La	57	24s22p14d10f2g
Yb	70	26s21p14d10f2g
Hg	80	25s21p15d10f2g
Pb	82	25s22p16d10f2g
Ra	88	26s23p16d11f2g

^a augmented by 2 high exponent s and 4 high exponent p functions.

units ($|e| = 1, \hbar = 1, m_e = 1$), the single electron DHF Hamiltonian is given by

$$\hat{H}_0 = c\boldsymbol{\alpha} \cdot \mathbf{p} + (\beta - 1)c^2 - \frac{Z}{r} + V_e(r), \quad (7)$$

where $\boldsymbol{\alpha}$ and β are the Dirac matrices and $V_e(r)$ is the self-consistent DHF potential due to atomic electrons. In order to take into account the specifics of diatomic molecules, we use a slightly modified $V_e(r)$ potential compared to standard atomic techniques:

$$V_e(r) = V_{\text{DHF}}^{N-N_v} + \frac{N_v - 1}{\sqrt{r^2 + R_e^2}}. \quad (8)$$

Here $V_{\text{DHF}}^{N-N_v}$ is the self-consistent DHF potential of the closed-shell core of the heavy atom, N is total number of electrons in this atom ($N = Z$ for a neutral system), N_v is the number of valence electrons, r is the distance to the heavy nucleus, and R_e is the distance between the nuclei in the molecule. The second term in (8) represents the spherically symmetric contribution from the valence electrons that are assumed to be moved to the second atom. Its form is chosen to have the correct $-1/r$ asymptote for the total potential at large distances in the case of neutral molecule.

The self-consistent DHF procedure is first done for the ion, from which valence electrons are removed. Then the core potential $V_{\text{DHF}}^{N-N_v}$ is frozen and valence $s_{1/2}$ and $p_{1/2}$ states are calculated by solving the DHF equations for the valence electron

$$(\hat{H}_0 - \epsilon_v)\psi_v = 0, \quad (9)$$

where \hat{H}_0 is given by (7) and (8).

For example, in the case of the BaF molecule, $Z = N = 56$, $N_v = 2$, and $R_e = 2.162 \text{ \AA}$ [31]. The self-consistent DHF procedure is performed for the Ba^{2+} ion. The $6s_{1/2}$ and $6p_{1/2}$ valence states are calculated in the potential

$$V(r) = -\frac{56}{r} + V_{\text{DHF}}(\text{Ba}^{2+}) + \frac{1}{\sqrt{r^2 + R_e^2}}. \quad (10)$$

These $6s_{1/2}$ and $6p_{1/2}$ states are used in the denominator of (5).

2. Inclusion of electron correlation

We include two important classes of electron correlation corrections: the core polarization correction and the Brueckner-type correlations. These types of correlations dominate in $s_{1/2}$ and $p_{1/2}$ atomic states and their inclusion leads to an accuracy of a few percent for the matrix elements [43].

The core polarization can be understood as the change of the self-consistent DHF potential due to the effect of the extra term (the weak interaction operator \hat{H}_A) in the Hamiltonian. The inclusion of the core polarization in a self-consistent way is equivalent to the well-known random-phase approximation (RPA) (see, e.g. [43]). The change of the DHF potential is found by solving the RPA-type equations self-consistently for all states in the atomic core. The RPA equations have a form of the DHF equations with the right-hand side:

$$(\hat{H}_0 - \epsilon_c)\delta\psi_c = (-\hat{H}_A + \delta V_A)\psi_c, \quad (11)$$

where \hat{H}_0 is the DHF Hamiltonian (7), index c enumerates states in the core, $\delta\psi_c$ is the correction to the core state c due to weak interaction \hat{H}_A , and δV_A is the correction to the self-consistent core potential due to the change of all core functions. Once δV_A is found, the core polarization can be included into a matrix element for valence states v and w via the redefinition of the weak interaction Hamiltonian,

$$\langle v|\hat{H}_A|w\rangle \rightarrow \langle v|\hat{H}_A + \delta V_A|w\rangle. \quad (12)$$

We then obtain the scaling parameter for core polarization, K_{CP} , from

$$K_{CP} = \frac{\langle \psi_{ns_{1/2}}^{\text{DHF}}|\hat{H}_A + \delta V_A|\psi_{n'p_{1/2}}^{\text{DHF}}\rangle}{\langle \psi_{ns_{1/2}}^{\text{DHF}}|\hat{H}_A|\psi_{n'p_{1/2}}^{\text{DHF}}\rangle}. \quad (13)$$

The values of K_{CP} for all the atoms under study are presented in Table IV.

In contrast to the core polarization correction, which can be reduced to the redefinition of the interaction Hamiltonian, the Brueckner-type correlations can be reduced to the redefinition of the single-electron orbitals, by replacing the DHF orbitals by the Brueckner orbitals

(BO). Brueckner correlations describe the interaction between the valence and the core electrons. These correlations can be included with the use of the so-called correlation potential $\hat{\Sigma}$, which is defined in such a way that the average value of $\hat{\Sigma}$ over a valence state v is the correlation correction to the energy of this state:

$$\delta\epsilon_v = \langle v|\hat{\Sigma}|v\rangle. \quad (14)$$

The correlation potential $\hat{\Sigma}$ is a non-local operator similar to the DHF exchange potential. It can be calculated by means of the many-body perturbation theory (MBPT) in the residual electron-electron Coulomb interaction. The expansion starts from second order in this interaction and in most cases this is the leading term. We use the B-splines in a box [44] and the second-order MBPT to calculate $\hat{\Sigma}$. The Brueckner orbitals for the valence states are found by solving the DHF-like equations with an extra operator $\hat{\Sigma}$ included:

$$(\hat{H}_0 + \hat{\Sigma} - \epsilon_v)\psi_v^{\text{BO}} = 0. \quad (15)$$

Solving these equations gives new energies and new wave functions for the valence states. For all atoms considered in present paper the inclusion of the second-order correlation potential $\hat{\Sigma}$ leads to a few percent accuracy for the energies of the $s_{1/2}$ and $p_{1/2}$ states. Matrix element of the operator \hat{H}_A between valence states v and w , in which both type of correlations are included, is given by

$$\langle \psi_v^{\text{BO}}|\hat{H}_A + \delta V_A|\psi_w^{\text{BO}}\rangle. \quad (16)$$

The K_W factor (Eq. (5)) is then reduced to

$$K_W = \frac{\langle \psi_{ns_{1/2}}^{\text{BO}}|\hat{H}_A + \delta V_A|\psi_{n'p_{1/2}}^{\text{BO}}\rangle}{\langle \psi_{ns_{1/2}}^{\text{DHF}}|\hat{H}_A|\psi_{n'p_{1/2}}^{\text{DHF}}\rangle}. \quad (17)$$

An additional effect of correlation, not taken into account in the above is the change in the expansion coefficients a, b, c, \dots in Eq. (4). In order to treat this effect we turn to the following expression,

$$\frac{\langle ns_{1/2}|H_A|np_{1/2}\rangle \langle np_{1/2}|E1|ns_{1/2}\rangle}{E_{ns_{1/2}} - E_{np_{1/2}}}. \quad (18)$$

Such an expression appears in atomic parity violating electromagnetic amplitudes and, in addition to the weak matrix element, it contains the $E1$ amplitude and the energy denominator between the s and the $p_{1/2}$ states. In molecules, use of this expression may be justified by the ionic bond model, where the electron that moves to the halogen polarizes the metal atom and produces a mixture of s and p orbitals. Table IV contains the obtained K_W (corresponding to $\langle ns|H_A|np\rangle$), along with K_{E1} and K_{E_n} factors, which describe the effects of core polarization (Eq. (11)-(12)), and the correlations (Eqs. (14)-(17)) on the $E1$ amplitude and the energy denominator, respectively. The final rescaling parameter K_{tot} is the product of all three factors

$$K_{tot} = K_W \cdot K_{E1} \cdot K_{E_n}. \quad (19)$$

TABLE IV. K_{CP} , K_W , K_{E1} , K_{E_n} , and K_{tot} correlation scaling factors for the atoms under study.

Atom	K_{CP}	K_W	K_{E1}	K_{E_n}	K_{tot}
Mg	1.24	1.38	0.97	0.96	1.29
Ca	1.28	1.54	0.91	0.90	1.26
Zn	1.12	1.38	0.87	0.91	1.09
Br	1.31	2.41	0.84	0.80	1.34
Sr	1.26	1.60	0.88	0.86	1.21
Zr	1.20	1.40	0.88	0.91	1.12
Cd	1.11	1.40	0.80	0.86	0.96
Ba	1.26	1.69	0.84	0.82	1.16
La	1.22	1.54	0.85	0.86	1.13
Yb	1.20	1.63	0.83	0.83	1.12
Hg	1.09	1.33	0.74	0.86	0.85
Pb	1.10	1.22	0.77	0.95	0.89
Ra	1.22	1.64	0.91	0.81	1.21

The final K_{tot} factors can be found in Table IV, and are used to scale the DHF W_A parameters to include the effects of electron correlation. (Note that that for PbF we have calculated only correlations between the valence electrons and the Pb core; the correlations between the valence electrons $6s$ and $6p$ are not included and should be treated separately using a different technique). The remaining correlation corrections, which are often called the weak correlation potential $\delta\Sigma_A$ or structural radiation, are suppressed by a small ratio $\epsilon_v/\epsilon_c \sim 0.1$, where ϵ_v is the valence electron energy and ϵ_c is the core electron energy. The effect of $\delta\Sigma_A$ usually does not exceed a few percent [45, 46].

- [1] Y. B. Zeldovich, *Sov. Phys. JETP* **6**, 1184 (1958).
- [2] O. P. Sushkov, V. V. Flambaum, and I. B. Khriplovich, *Sov. Phys. JETP* **60**, 873 (1984).
- [3] C. S. Wood, S. C. Bennett, D. Cho, B. P. Masterson, J. L. Roberts, C. E. Tanner, and C. E. Wieman, *Science* **275**, 1759 (1997).
- [4] V. V. Flambaum and I. B. Khriplovich, *Sov. Phys. JETP* **52**, 835 (1980).
- [5] W. C. Haxton, C.-P. Liu, and M. J. Ramsey-Musolf, *Phys. Rev. C* **65**, 045502 (2002).
- [6] J. S. M. Ginges and V. V. Flambaum, *Phys. Rep.* **397**, 63 (2004).
- [7] V. N. Novikov, O. P. Sushkov, V. V. Flambaum, and I. B. Khriplovich, *Sov. Phys. JETP* **46**, 420 (1977).
- [8] V. V. Flambaum and I. B. Khriplovich, *Sov. Phys. JETP* **62**, 872 (1985).
- [9] V. V. Flambaum, I. B. Khriplovich, and O. P. Sushkov, *Phys. Lett. B* **146**, 367 (1984).
- [10] V. V. Flambaum and D. W. Murray, *Phys. Rev. C* **56**, 1641 (1997).
- [11] P. A. Vetter, D. M. Meekhof, P. K. Majumder, S. K. Lamoreaux, and E. N. Fortson, *Phys. Rev. Lett.* **74**, 2658 (1995).
- [12] L. N. Labzovsky, *Sov. Phys. JETP* **48**, 434 (1978).
- [13] O. P. Sushkov and V. V. Flambaum, *Sov. Phys. JETP* **48**, 608 (1978).
- [14] V. V. Flambaum and I. B. Khriplovich, *Phys. Lett. A* **110A**, 121 (1985).
- [15] D. DeMille, S. B. Cahn, D. Murphree, D. A. Rahmlow, and M. G. Kozlov, *Phys. Rev. Lett.* **100**, 023003 (2008).
- [16] J. Thyssen, *Development and Applications of Methods for Correlated Relativistic Calculations of Molecular Properties*, Dissertation, Department of Chemistry, University of Southern Denmark, Odense, Denmark (2001).
- [17] T. Saue and T. Helgaker, *Journal of Computational Chemistry* **23**, 814 (2002).
- [18] T. Saue, K. Fægri, T. Helgaker, and O. Gropen, **91**, 937 (1997).
- [19] T. Saue and H. J. Aa. Jensen, *J. Comp. Phys.* **111**, 6211 (1999).
- [20] DIRAC, a relativistic ab initio electronic structure program, Release DIRAC10 (2010), written by T. Saue, L. Visscher and H. J. Aa. Jensen, with contributions from R. Bast, K. G. Dyall, U. Ekström, E. Eliav, T. Enevoldsen, T. Fleig, A. S. P. Gomes, J. Henriksson, M. Iliaš, Ch. R. Jacob, S. Knecht, H. S. Nataraj, P. Norman, J. Olsen, M. Pernpointner, K. Ruud, B. Schimmelpfennig, J. Sikkema, A. Thorvaldsen, J. Thyssen, S. Villaume, and S. Yamamoto (see <http://dirac.chem.vu.nl>).
- [21] L. Visscher, T. Saue, and J. Oddershede, *Chemical Physics Letters* **274**, 181 (1997).
- [22] L. Visscher and K. G. Dyall, *Atom. Data Nucl. Data Tabl.* **67**, 207 (1997).
- [23] C. Thierfelder, G. Rauhut, and P. Schwerdtfeger, *Phys. Rev. A* **81**, 032513 (2010).
- [24] R. A. Kendall, T. H. Dunning, and H. R. J., *J. Chem. Phys.* **96**, 6796 (1992).
- [25] D. E. Woon and T. H. Dunning, *J. Chem. Phys.* **98**, 1358 (1993).
- [26] K. Faegri, *Theor. Chim. Acta* **105**, 252 (2001).
- [27] J. K. Laerdahl and P. Schwerdtfeger, *Phys. Rev. A* **60**, 4439 (1999).
- [28] L. Visscher, T. J. Lee, and K. G. Dyall, *J. Comp. Phys.* **105**, 8769 (1996).
- [29] M. Iliaš, H. J. A. Jensen, V. Kello, B. O. Roos, and M. Urban, *Chem. Phys. Lett.* **408**, 210 (2005).
- [30] M. Iliaš and T. Saue, *J. Comp. Phys.* **126**, 064102 (2007).
- [31] K. Huber and G. Herzberg, in *NIST Chemistry WebBook*, NIST Standard Reference Database No. 69, edited by P. Linstrom and W. Mallard (National Institute of Standards and Technology, Gaithersburg MD, 2011) <http://webbook.nist.gov>.
- [32] M. Nayak and B. Das, *Phys. Rev. A* **79** (2009).
- [33] M. G. Kozlov, A. V. Titov, N. S. Mosyagin, and P. V. Souchko, *Phys. Rev. A* **56**, R3326 (1997).
- [34] M. G. Kozlov and L. N. Labzovsky, *J. Phys. B* **28**, 1933 (1995).
- [35] A. V. Titov, N. S. Mosyagin, and V. F. Ezhov, *Phys. Rev. Lett.* **77**, 5346 (1996).
- [36] Y. Y. Dmitriev, Y. G. Khait, M. G. Kozlov, L. N. Labzovsky, A. O. Mitrushenkov, A. V. Shtoff, and A. V. Titov, *Physics Letters A* **167**, 280 (1992).
- [37] M. Kozlov, V. Fomichev, Y. Dmitriev, L. Labzovsky, and A. Titov, *J. Phys. B* **20**, 4939 (1987).

- [38] K. I. Baklanov, A. N. Petrov, A. V. Titov, and M. G. Kozlov, *Phys. Rev. A* **82**, 060501(R) (2010).
- [39] T. A. Isaev, S. Hoekstra, and R. Berger, *Phys. Rev. A* **82**, 052521 (2010).
- [40] K. E. Banyard and M. R. Hayns, *J. Phys. Chem.* **75**, 416 (1971).
- [41] M. A. Flory, S. K. McLamarrah, and L. M. Ziurys, *J. Chem. Phys.* **125**, 194304 (2006).
- [42] J. Autschbach, S. Siekierski, M. Seth, P. Schwerdtfeger, and W. H. E. Schwarz, *J. Comput. Chem.* **23**, 804 (2002).
- [43] V. A. Dzuba, V. V. Flambaum, P. G. Silvestrov, and O. P. Sushkov, *J. Phys. B* **20**, 1399 (1987).
- [44] W. R. Johnson and J. Sapirstein, *Phys. Rev. Lett.* **57**, 1126 (1986).
- [45] V. A. Dzuba, V. V. Flambaum, P. G. Silvestrov, and O. P. Sushkov, *Phys. Scr.* **36**, 69 (1987).
- [46] V. A. Dzuba, V. V. Flambaum, and O. P. Sushkov, *Phys. Lett. A* **141**, 147 (1989).